Fast, Mathematically Exact *k*-Space Sample Density Compensation for Rotationally Symmetric Interleaved Trajectories, and the SNR-Optimized Reconstruction from non-Cartesian Samples

D. Mitsouras[1], R. V. Mulkern[1,2], and F. J. Rybicki[1]

[1]Radiology, Harvard Medical School & Brigham And Women's Hospital, Boston, MA, United States, [2]Radiology, Children's Hospital, Boston, MA, United States

Introduction: The problem of density compensation of non-uniformly arranged *k*-space samples has been extensively studied [1-8]. Popular solutions involve heuristic arguments such as assigning a *k*-space area to each sample [3] in an attempt to mimic the implicit Jacobian [4], or, goal-based iterative optimization of the point-spread function based on the convolution kernel [5] used in gridding [1,2]. A recently developed method for exact density compensation solves a system of equations based on the analytically known cross-correlations (CC) of the Fourier basis functions underlying the *k*-space trajectory [6]. The solution to this system of equations represents compensated samples that normalize the contribution of each *independent* information element that has been captured by the *k*-space trajectory. Unfortunately, this and other linear-system based image reconstruction approaches [7-8] become computationally debilitating with increasing image resolution [7-8]. For example, density compensation of samples acquired for a 256 image matrix requires solving a system of equations sized appx. 65000-by-65000. Here it is shown for the first time that when a trajectory is composed of rotationally symmetric interleaves, such as multi-shot spiral and PROPELLER [9] trajectories, the CC method leads to a highly simplified circulant block-Toeplitz system matrix that is easily block-diagonalized by application of a *n*-point DFT where *n* is the number of interleaves. In contrast to typical methods for density compensation [1-5] that limit the interactions considered via e.g., a kernel of limited extent, the CC method considers *all* interactions between *all* samples, affording it both increased accuracy as well as the ability to exploit any redundancy in sampling [6]. In the context of image reconstruction it is shown that the latter can be used to increase SNR. The development of this method provides these advantages with reconstruction times of the order of a few seconds.

Theory: The CC method [6] showed that the density compensated vector of *k*-space samples **x** solves the linear system **Ax=b** where the vector **b** contains the acquired *k*-space samples and the entries of the matrix **A** are the cross-correlations of the Fourier basis functions corresponding to the *k*-space locations visited by the trajectory. For a trajectory such as spiral, PROPELLER and radial, where the design FOV is a disk, the entries of **A** are [6] $\mathbf{A}_{j,l} = \int_R \left(f_j(\vec{r})\right)\left(f_l(\vec{r})\right)^* d\vec{r} = \left(2\left|\left(\vec{k}_j - \vec{k}_l\right)\right|\right)^{-1} J_1\left(\pi\left|\left(\vec{k}_j - \vec{k}_l\right)\right|\right)$, where $f_j(\vec{r}) = e^{-i2\pi\vec{k}_j \cdot \vec{r}^T}$ is the Fourier basis function corresponding to the *j*th *k*-space location $\vec{k}_j$, $J_1(\cdot)$ is the Bessel function of the first kind, and the superscripts * and T denote Hermitian conjugate and transposition respectively. For a trajectory composed of *n* rotationally symmetric interleaves each composed of *m* samples, the rows of the matrix **A** can be arranged such that the first *m* rows correspond to the first interleave, the second set of *m* rows correspond to the second interleave and so forth, so that the matrix **A** can be written as $\mathbf{A} = \begin{bmatrix} \mathbf{C}^{1,1} & \cdots & \mathbf{C}^{1,n} \\ \vdots & \ddots & \vdots \\ \mathbf{C}^{n,1} & \cdots & \mathbf{C}^{n,n} \end{bmatrix}$, where the *m* by *m* sub-matrices $\mathbf{C}^{a,b}$ contain the cross correlations between the elements of interleave *a* and those of interleave *b*. Because the cross-correlations depend only on the *k*-space distance between two samples (the argument $\left|\left(\vec{k}_j - \vec{k}_l\right)\right|$ in the respective equation), if the interleaves are rotationally symmetric and separated by a fixed angle, then the distance between a sample *j* on interleave *a* and a sample *l* on interleave *b* is the same as the distance between sample *j* on the first interleave and sample *l* on the interleave that is as many interleaves away from the first one as *b* is from *a*. That is, $\mathbf{C}^{a,b} \equiv \mathbf{C}^{1,b-a+1}$. In addition, the cross-correlations matrix **A** is symmetric by construction. Using these two facts, the matrix **A** is revealed to be circulant block-Toeplitz. For example, for a trajectory composed of 6 rotationally symmetric segments, the matrix **A** has the form shown in Eq.[1]. Such a matrix is composed of $\lfloor n/2 \rfloor + 1$ different sub-matrices of size *m* by *m*, and is block-diagonalized by a *n* point DFT so that a linear system based on this *nm* by *nm* system matrix **A** can be solved by solving *n* individual linear systems of size only *m* by *m* [10]. For example, samples acquired using a 32-way interleaved spiral trajectory can be compensated by solving 32 linear systems each of size e.g., 2048 by 2048, which can be solved in as little as 6 sec.

$$\mathbf{A} = \begin{bmatrix} \mathbf{C}^{1,1} & \left(\mathbf{C}^{1,2}\right)^T & \cdots & \mathbf{C}^{1,2} \\ \mathbf{C}^{1,2} & \mathbf{C}^{1,1} & \cdots & \mathbf{C}^{1,3} \\ \mathbf{C}^{1,3} & \mathbf{C}^{1,2} & \cdots & \left(\mathbf{C}^{1,3}\right)^T \\ \left(\mathbf{C}^{1,3}\right)^T & \mathbf{C}^{1,3} & \cdots & \left(\mathbf{C}^{1,2}\right)^T \\ \left(\mathbf{C}^{1,2}\right)^T & \left(\mathbf{C}^{1,3}\right)^T & \cdots & \mathbf{C}^{1,1} \end{bmatrix} \qquad \textbf{Eq.[1]}$$

Methods: Experiments were performed on a 1.5T MR scanner (GE Medical Systems, Milwaukee, WI) equipped with 4G/cm, 15 G/cm/ms gradients, and using a quadrature head coil. Simulations were performed assuming the same. For simulations, a 32-way interleaved spiral designed for 256 image matrix and 18 cm FOV (1744 samples per interleave) was used to simulate acquisition of the modified Shepp-Logan phantom. For experiments the scanner-supplied GRE spiral sequence was used to acquire a QA phantom using a 32-way interleaved acquisition (2048 samples per interleave) with 14 cm FOV, 45^o flip angle, 2.5 ms TE, and 150 ms TR. Each simulation and experiment was repeated 2000 times to assess SNR performance; simulations were performed with random noise added while the experiment was repeated under identical measurement conditions. Reconstruction error was computed for the simulations using the normalized root-mean-square error (NRMSE). SNR was measured for both simulations and experiments using a) mean values within signal and noise ROIs and b) using the standard deviation of individual pixels over the 2000 repetitions of the simulations and experiment. Standard block-diagonalization of the circulant block-Toeplitz system matrix was used [10] to solve the 32 independent linear systems required to reconstruct each image. Each system required appx. 6 sec to solve *non-iteratively* using Matlab (Mathworks, Natick, MA). A simple regularization was used to constrain the amplitude of the compensated samples. Given that the CC matrix for spiral trajectories has a large sub-space with small eigenvalues [6], multiple solutions to the density compensation problem exist. This fact has been used to e.g., choose different RF fields (in 2D RF excitation on a given spiral) that produce the same excitation profile but have differing characteristics such as power deposition [11] or field smoothness [6]. The scheme used here chooses solutions with different SNR characteristics of the reconstructed image. The Voronoi [3] and Pipe & Menon density compensation methods were used for comparison.

Results: The mean NRMSE and SNR over 2000 simulations performed for the modified Shepp-Logan phantom (normalized to maximum value of 1), with each simulation containing a different set of random noise samples drawn from a normal distribution of standard deviation equal to12% of the phantom's energy, are provided in the Table. Also provided is the standard deviation (STD) of a pixel's value, arbitrarily chosen from the signal ROI. As shown, NRMSE is 10.6% lower and SNR is 28.5% higher for the CC method compared to Voronoi and Pipe & Menon density compensation. Similar to SNR, STD is 21.2% lower. Experimental results are summarized in Fig. 1, and show a similar increase of 36.3% SNR increase for one of the reconstructed images, and 26.6% reduction in STD of a signal ROI pixel's value over 2000 experiment repetitions.

Noise	Method	NRMSE (%)	SNR	STD
12%	Voronoi	19.64	14.35	0.0558
	Pipe & Menon	19.63	14.39	0.0558
	Cross-Correlations	17.56	18.44	0.0440

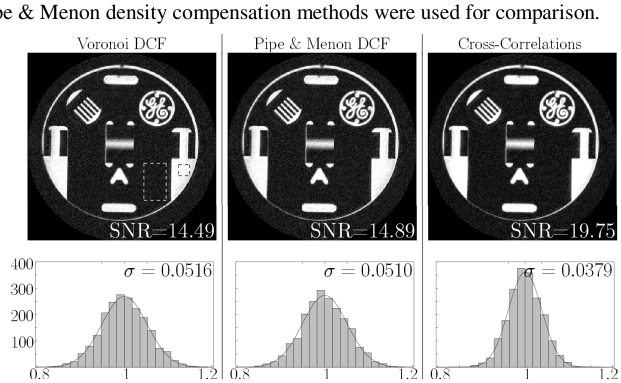

Figure 1 Top row: example image (of 2000) acquired using a 32-way interleaved spiral trajectory (256 matrix) reconstructed using different density compensation methods. SNR was computed using the signal and noise ROIs shown with dashed lines on left image. Bottom row: Histograms of the 2000 reconstructed values of a pixel arbitrarily chosen in the signal ROI for the respective method.

Conclusions: A mathematically exact density compensation method that considers all interactions between all samples was shown to be easy to solve for rotationally symmetric interleaved trajectories. By exploiting the multitude of interactions in a spiral trajectory, the method achieved reconstruction error reduction by 10% concurrently with a 28.5% SNR increase in simulation compared to popular methods. A 36.3% SNR increase was shown experimentally.

Acknowledgements: Whitaker Foundation, NIH K23-EB00882. **References:** [1] O'Sullivan JD, IEEE TMI 1985;4:200-7. [2] Jackson JI et al, IEEE TMI 1991;10:473-8. [3] Rasche V et al, IEEE TMI 1999;18:385-92. [4] Lauzon ML et al, MRM 1996;36;940-9. [5] Pipe JG et al, MRM 1999;41:179-86. [6] Mitsouras D et al, MRM 2007;57:338-52. [7] Van De Walle R et al, IEEE TMI 2000;19:1160-7. [8] Desplanques B et al, IEEE Trans Nuc Sci 2002;49:2268-73. [9] Pipe JG, MRM 1999;42:963-9. [10] Davis P, Circulant Matrices, Chelsea Publications, 2nd ed., 1994. [11] Yip CY et al, MRM 2005;54:908-17.